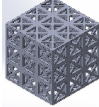



## P2 Porous Structure Test Report #2 - Simulations

Team 25, ConcussionZero, Eric Strathdee

Date: 16/03/31

Structure ID: BCC/FCC V3 (TPU)

Design Criterion	Target	Modelled Result		Experimental Result		Percent Difference
Porous Structure			y/n		y/n	
Bulk width [mm]	30	30	Y	29.89	Y	0.37%
Bulk breadth [mm]	30	30	Y	29.91	Y	0.30%
Bulk Length [mm]	30	30	Y	29.9	Y	0.33%
Bulk Volume [mm <sup>3</sup> ]	minimize	27000		26730.9		1.01%
Material Volume [mm <sup>3</sup> ]	minimize	7413.89	Y	9000	Y	-17.6%
Pore Volume [mm <sup>3</sup> ]	maximize	19586.11	Y	17730.9	Y	10.5%
Porosity [%]	maximize	72.54	Y	66.33	Y	9.36%
Mass [g]	minimize	7.99	Y	7.99	Y	0%
Deflection, under 59 N static load [mm]	2-5	0.5007	N	0.5	N	0.14%
Structural Stiffness, under 59 N static load [N/mm]	10-24	118.64	N	118.8	N	-0.13%
Apparent Material Stiffness, Static [MPa]		3.955		3.97		-0.37%
Maximum Stress, under 50 N static load [MPa]	< 15.6	1.504	Y	Didn't Break	Y	-
Deflection at min drop height [mm]	10-16	4.473	N	4.5	N	-0.6%
Acceleration at min drop height [m/s <sup>2</sup> ]	< 160	219.32	N	77.2	Y	185.23%
Impact Force at min drop height [N]	< 388	530.68	N			
Rebound Height [mm]		8		8		0%
Rebound/Drop Height		0.16		0.16		0%

Maximum Stress, under dynamic load [MPa]	< 15.6	1.026	Y	Didn't Break	Y	-
Max Drop Height [m]	maximize	0.067				

### Design Notes:

#### Design:

The design of the shock absorbent structure consisted of repeating crystalline structures set up in orderly fashion to create a stiff, porous structure. Various unit cell designs for this lattice structure were constructed and simulated, such as rhombicuboctahedrons, face-centered cubic cells (FCC), body centered cubic cells (BCC), as well as more cylindrical and hexagonal designs. The decided upon design, which was selected after in depth simulation and analysis, was a combination of the FCC and BCC crystalline structures. The BCC structure proved capable of withstanding stress while maintaining porosity due to its interior struts, as seen in Figure 1.

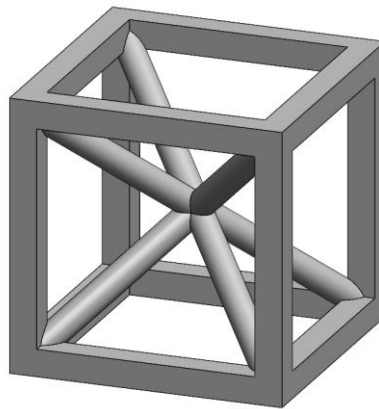


*Figure 1: A dimetric view of a designed 10mm-by-10mm-by-10mm BCC unit cell.*

The characteristics of the BCC unit cell were desirable when designing the lattice, however, to improve the strength and stiffness of the structure, the 'x' pattern of the FCC was implemented, as seen in Figure 2.

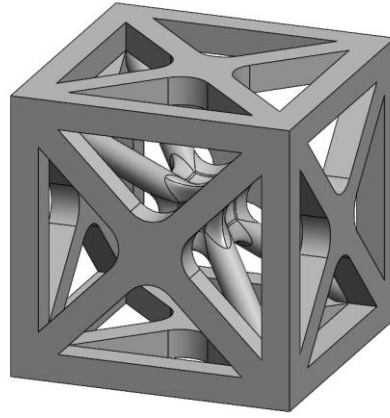


*Figure 2: A dimetric view of the designed 10mm-by-10mm-by-10mm unit cell used in the 3D-printed lattice structure.*

By adding the FCC components to the design, the cross-sectional area of the structure was increased throughout, meaning that the stress on the structure during testing could be reduced when compared to just the BCC structure. This 'x' pattern also encouraged more vertical stiffness in the structure, to prevent fracturing at the sides. The addition of fillets seen in Figure 2 also helped to reduce stress concentrations found at sharp corners and cross-sections, such as the internal struts and the FCC pattern. Each part of the unit cell consisted of a 1mm thickness, such as the outer walls or the strut diameter. The test structure to be printed allowed for maximum dimensions of 30mm-by-30mm-by-30mm, so this unit cell design was repeated 3 times in multiple directions, creating a cubic lattice structure as seen in Figure 3.

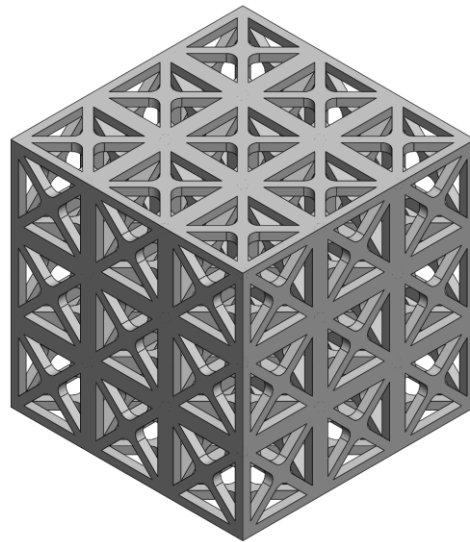


*Figure 3: An isometric view of the complete 30mm-by-30mm-by-30mm lattice, comprised of FCC/BCC unit cells.*

The lattice was consistent throughout its design, due to the repetition of the original unit cell. As determined through SolidWorks and calculations, the cubic lattice was able to maximize porosity as well as structural strength but allowed for less deflection than other designs. One potential flaw not accounted for when creating the lattice was the bulkier walls generated because of repeating the unit cells. Due to their general cubic dimensions of 10mm, when made

to fit the exact bulk dimensions ( $27000\text{mm}^3$ ), the walls connecting each unit cell in the middle sections were 2mm in thickness. This thickness resulted in less compressible components in the centre of the lattice which would explain the lower deflection, as these thicker areas resulted in a higher stiffness. The design was originally created to be printed from Tango Black; however, simulations were run for a TPU material as well. A simulation for TPU material is shown in Figure 4.

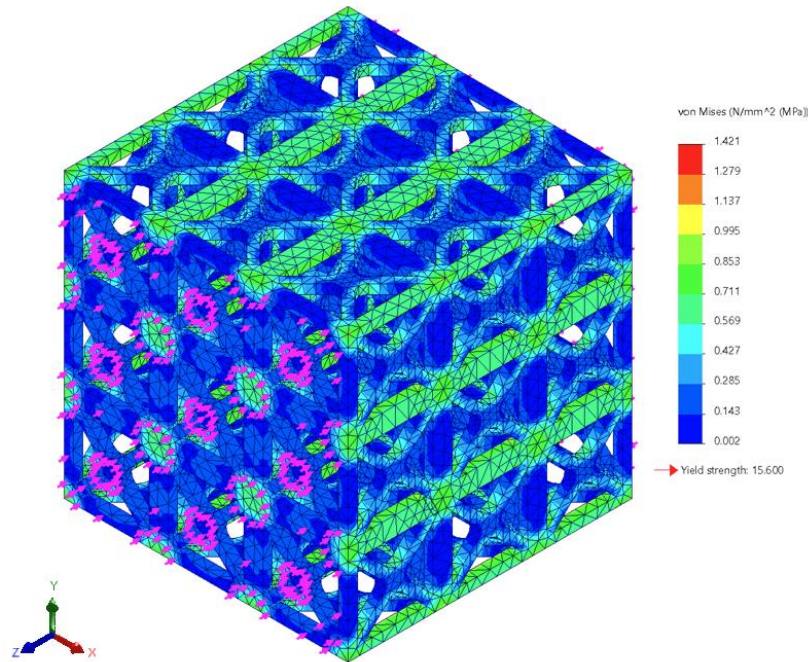


Figure 4: Von Mises stress of lattice structure under a 50N static load (pink arrows). Yield stress of 15.6 MPa, structural stiffness of 37.62N/mm, apparent material stiffness of 1.254 MPa, deflection of 1.329mm, assumed Poisson's Ratio of 0.49.

The simulation for the TPU lattice revealed that the thicker areas with higher stiffness were subject to greater stress concentrations due to their immobility. The green sections in Figure 4 represent this higher value of stress, and it is mostly focused at the 2mm thick column like features of the lattice. Although there are concentrated areas of stress, the maximum stress reached in simulation was 1.421 MPa, well below the yield, implying that the structure would not fracture under 50N. Overall, the design was able to meet most of the requirements, except for it being slightly too stiff. The next step in the process was to 3D-print the design for testing, and it was printed in both TangoBlack and TPU.

### Testing and Results:

Due to complications with the support material in the TangoBlack lattice structure, the testing was conducted only on the TPU material. The TangoBlack test sample was more elastic than the TPU sample, but the presence of support material within the TangoBlack lattice would have returned results which would not have been able to be reasonably applied to the designed lattice. The TPU structure was significantly closer to the modeled design, and so testing results would be similar and could allow for adjustments to the material property settings.

The passive properties of the lattice structure, such as the volume, mass, and dimensions, were obtained through 3 different tests. The volume of the structure was determined through fluid displacement, the mass was measured directly on a scale, and the bulk dimensions were obtained using a vernier caliper. The fluid displacement test was used to measure the volume to account for the porosity of the structure. For this test, 1 mL was taken to be equivalent to 1000 mm<sup>3</sup>.

Both static and dynamic testing was conducted on the TPU lattice structure. The results of these tests allowed for more accurate material property values to be obtained. A more accurate understanding of the behaviour of the material will increase the reliability of further FEA analyses on future design iterations.

The static testing consisted of placing various weights onto the structure and measuring the displacement of the lattice. A total of 5 weights ranging from 1.2 to 6.0 kg were used. To measure the deflection, a clear hollow cylinder with a tape measure was placed over the weight and lattice structure. Photographs were taken of the lattice under load. The deflection data obtained is shown in Table 1.

*Table 1: Measured deflections of the lattice structure under various static loads.*

<b>Weight (N)</b>	<b>Measured Deflection (mm)</b>
0	0
12.3	0
23.5	0
35.8	0
47.1	0.25
59.4	0.5

As the static testing conducted failed to measure the lateral strain of the lattice, used to calculate a more accurate Poisson's ratio, further static testing was conducted. A 20 lb (88 N) dumbbell was used as the weight, and a ruler was used to measure the axial and transverse strain of the lattice. The upper and lower portions of the lattice experienced different strains, so the average of the two values was used. A photo of this static testing is shown in Figure 5.



Figure 5: Photo of the setup of the secondary static test used to determine the Poisson's ratio of the material.

As this test was conducted without the use of a bracing structure to prevent the dumbbell from falling off the structure, external force was used to hold the weight in place, potentially reducing the force on the structure. The weight of the dumbbell could not be calculated directly and was assumed to be exactly 20 lbs. Slight variations in this weight would reduce the accuracy of the tests. The strain data is shown in Table 2.

Table 2: Strain data determined through the secondary static testing

Weight (N)	Initial Height (mm)	Axial Deflection (mm)	Axial Strain (mm/mm)	Initial Width (mm)	Transverse Deflection (mm)	Transverse Strain (mm/mm)
88	28	-4	-0.143	29	+2	0.069

The dynamic testing involved dropping a 2.4 kg mass onto the structure from a height of 50 mm. An accelerometer secured to the top of the mass was used to determine the acceleration of the mass during impact. The accelerometer used a software called WitMotion. During testing, the data acquisition rate of the software was determined to be insufficient to capture the acceleration of the block. The maximum acceleration was therefore determined using the graphical display in the app. The figures used to obtain these values can be seen in

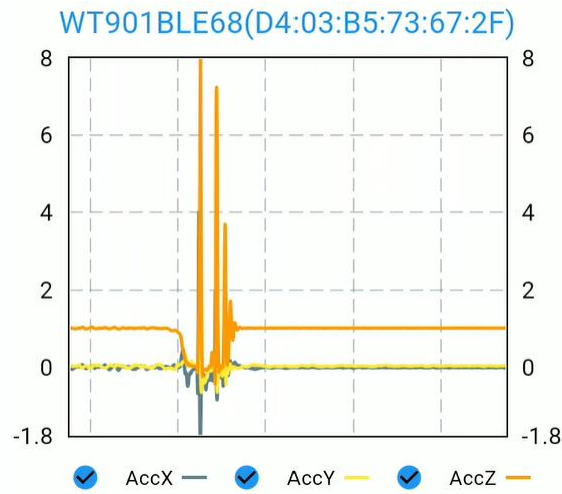


Figure 6: The instantaneous WitMotion acceleration plot (g's) acquired during testing.

The deflection of the structure was determined using video recordings of the testing. A clear hollow cylinder with a tape measure was placed over the mass to ensure a more accurate displacement measurement. The accuracy of the data was limited by the framerate of the camera, and thus not all trials could be used to measure the structures dynamic displacement. One of the trials, shown in Figure 7, successfully captured the mass at its lowest point, measured at the bottom of the faded and blurry region below the mass. The measured displacement based on this trial was determined to be 3 mm. Note that the block started at a measured height of 29 mm on the tape measure.

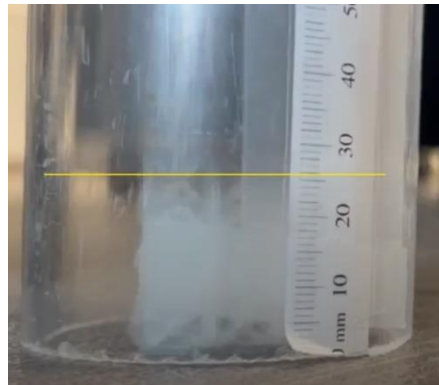


Figure 7: Maximum displacement of the lattice structure with a drop of 50 mm. The final height of the mass was determined to be the faded and blurry region underneath the opaque portion of the mass

The acceleration data for 3 drop-test trials are shown in Table 3. The maximum acceleration was taken using the acceleration graphs under the ACC tab in the WitMotion application.

Table 3: Calculated maximum acceleration ( $m/s^2$ ) over 3 separate drop test trials from a height of 50 mm.

Trial	Maximum Acceleration ( $m/s^2$ )
1	78.5
2	80.4
3	72.6



**Analysis:****Qualitative-**

The lattice structure did not fail under the static and dynamic testing. It was observed that the deformation of the lattice was not uniform but rather was concentrated at the bottom corner unit cells of the structure. The vertical supports on the outermost edge of the lattice displaced significantly under load; these portions of the lattice were observed to bulge outwards. The deformation can be seen in Figure 8, which shows the lateral strain of the structure under 88 N.



*Figure 8: Transverse deformation of the lattice structure under a 88 N load*

The uneven deformation behavior of the lattice structure could be attributed to the vertical supports present in the lattice structure. These supports were 2 times the thickness of the outer supports, resulting in a higher structural stiffness in these areas and in the overall structure.

Under dynamic loading, the lattice did not remain fixed to the floor but rather responded by briefly accelerating upwards with the mass. The lack of contact can be seen in Figure 9. The behaviour of the lattice could be attributed to the high elastic modulus calculated for the structure. A large elastic modulus would result in a significant amount of stored elastic energy, and as the lattice structure's mass is relatively small, this energy would likely be sufficient to cause the structure to accelerate upwards.

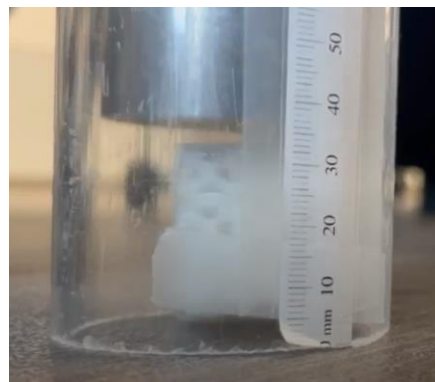


*Figure 9: Response of both mass and lattice structure after impact during dynamic testing*



During testing, the deformation of the lattice structure did not appear to follow a linear relationship. Up to a weight of 47.1 N, the deflection of the lattice structure was unmeasurable. The lattice's deformation began to be observable after 47.1 N and appeared to exhibit linear elastic behaviour up to the 59.4 N load. Once the 88 N load was applied, however, the deformation increased non-linearly. This behaviour can be seen in Figure 10. Since the lattice returned to its original shape after each loading, the 88 N load is still within the elastic response region of the lattice. Therefore, this point was still used to calculate the Poisson's ratio of the structure. However, since the SolidWorks modeling software assumes a linear elastic response, this 88 N data point will not be used for calculating an updated structural stiffness. The structural stiffness was instead calculated using the deformation under 59.4 N.

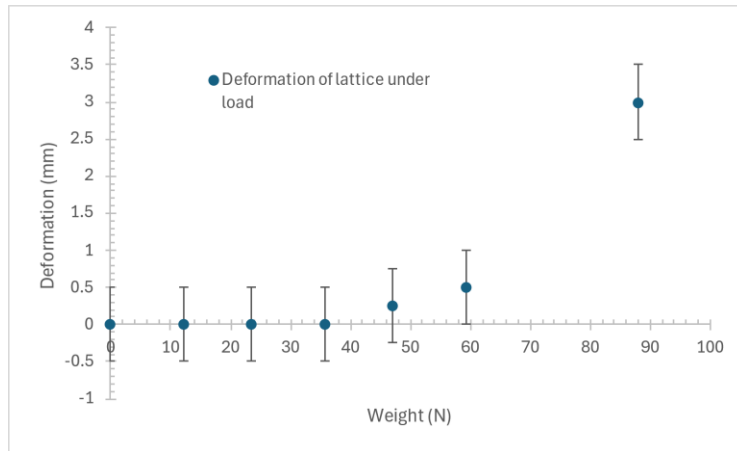


Figure 10: Deformation (in mm) of the lattice structure under load (in N)

The error in the deformation was taken to be half the smallest increment of the measurement device,  $\pm 0.5$  mm. This error is significant, as most of the measured deflections were under 1 mm. Due to time constraints and lack of equipment, re-testing was unable to be conducted. To improve the accuracy of the physical test results, more accurate measurement tools would be required.

### Quantitative-

The measured bulk dimensions of the lattice structure had less than 0.5% percent difference compared to the modeled. The small error may be due to thermal contraction of the filament as it solidifies during printing.

The calculated mass  $m$  (in grams) and volume  $V$  (in  $\text{cm}^3$ ) of the lattice structure was used to calculate the density of the lattice structure  $\rho$  (in  $\text{g}/\text{cm}^3$ ) using Equation 1.

$$\rho = \frac{m}{V} \quad (1)$$

The density was calculated to be  $0.888 \text{ g}/\text{cm}^3$ . FEA simulations run with this density resulted in a mass that was still significantly different from the measured mass of the TPU lattice. Linear interpolation was then used to arrive at a density that would yield the measured mass. This updated density was calculated to be  $1.078 \text{ g}/\text{cm}^3$ . This density is lower than the first assumption of  $1.134 \text{ g}/\text{cm}^3$ . The lower density may be attributed to the printer using less than

100% infill during printing, resulting in a lower density of material. The difference may also be attributed to printing errors. The 'x' pattern on the top surface of the lattice failed to print properly, as can be seen in Figure 11. The material used for these 'x' patterns likely remains on the structure, however, at a lower region in the lattice.



Figure 11: Top surface of the TPU lattice structure, highlighting the misprinting of the top 'x' patterns of the unit cells

The Poisson's ratio of the structure was calculated using the lattice's response under the 88 N load. Equation 2 was used to calculate Poisson's ratio  $\nu$  using the transverse and axial strain from Table 2 [1].

$$\nu = -\frac{\epsilon_{transverse}}{\epsilon_{axial}} \quad (2)$$

The Poisson's ratio was calculated to be 0.48, which is near to the assumed value based on the material data sheet of the TPU filament.

The static testing allowed for the calculation of the lattice's structural stiffness  $K$  (in N/mm) and the apparent elastic modulus  $E_{app}$  (in MPa). The stiffness of the lattice was determined to be 118.8 N/mm based on the deflection of the lattice under a 59.4 N load. Due to the large error in the values, the linear elastic region created using this point passes through the acceptable range of all the points up to 59.4 N. To determine the apparent material stiffness  $E_{app}$  of the 3D lattice, the structural stiffness  $K$  (in N/mm) of the test structure was normalized to the cross-sectional area  $A_{cross}$  (in mm<sup>2</sup>) and the length  $L$  (in mm). The  $E_{app}$  (in MPa) was calculated using Equation 3 below.

$$E_{app} = \frac{KL}{A_{cross}} \quad (3)$$

Using Equation 3, the  $E_{app}$  was determined to be 3.97, which is 3.17 times larger than the modelled value. The inconsistency between the modelled and measured values is significant and may be corrected by changing the material elastic modulus on SolidWorks. To correct for this difference, the previous elastic modulus of 15.3 MPa was multiplied by 3.17, resulting in an updated modulus of 48.3 MPa.

As energy conservation could not be assumed for the physical testing, the impact force on the lattice structure could not be calculated. During modeling, small deflections were assumed, which allowed for the impact force, dynamic deflection, and impact time to be calculated.

During physical testing, the lattice structure exhibited significant deflection, preventing the same assumption to be made.

The yield strength of the material was not updated as the physical testing was unable to determine the maximum stresses in the lattice. Since the lattice structure did not fail under the testing, the first assumption of the yield strength taken from the TPU material datasheet was kept.

The dynamic testing allowed for the calculation of the rebound/drop height. Figure 9 was used to obtain the maximum rebound height of the mass. It was determined that at a drop height of 50 mm, the mass had a rebound height of 8 mm. This resulted in a rebound/drop height percentage of 16%. This percentage is 2.88 times smaller than the assumed percentage of 46.1% based on external experiments [2] [3] [4] [5] [6]. The lower percentage could be attributed to losses from sound and friction between the mass and the hollow tube. Another source of error could be that the mass was not dropped from exactly 50 mm. If the mass was dropped from a lower height, at impact the mass would have less momentum which could be transferred to the lattice structure.

The important material properties, including density, Poisson's ratio, elastic modulus, yield strength and rebound/drop height ratio, are included in Table 4. Table 4 includes the values that were assumed based on material datasheets and in-class information, in addition to the updated values calculated after physical testing. The updated values were used to re-analyze the FEA of the TPU structure in SolidWorks in Figure 12.

*Table 4: Important properties of the TPU material, including initial assumptions based on datasheets and in-class information and post-testing updates*

<b>TPU</b>	<b>1<sup>st</sup> Assumption</b>	<b>Updated after testing</b>
Source	MatWeb [7] and In-Class Assumptions	Passive, Static, and Dynamic Testing
Density g/cm <sub>3</sub>	1.134	1.078
Poisson's Ratio	0.49	0.48
Elastic Modulus (MPa)	15.3	48.4
Yield Strength (MPa)	15.6	15.6
Rebound/Drop Height	46.1%	16%

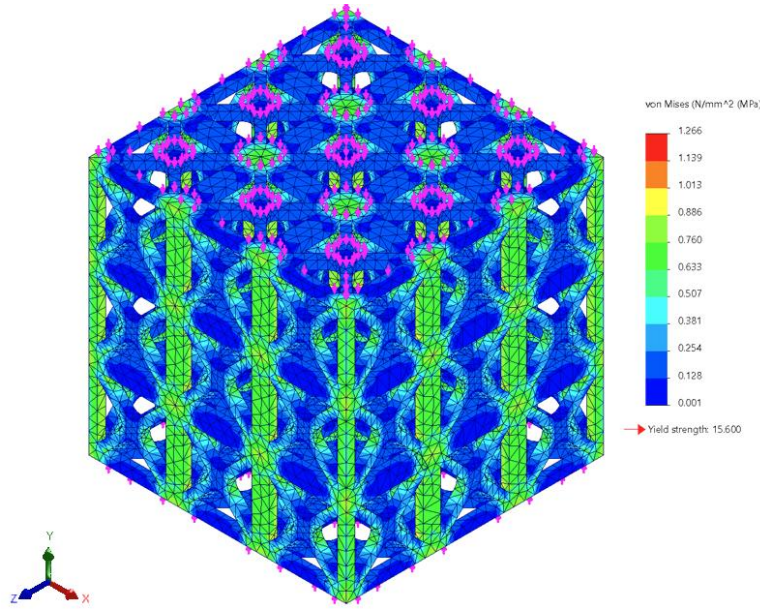


Figure 12: Von Mises stress of lattice structure under a 50N static load (pink arrows), using updated values from Table 4. Yield stress of 15.6 MPa, deflection of 0.4214mm.

After the FEA of the lattice was run again, the acceleration, displacement, and impact forces at the minimum drop height, in addition to the maximum stresses and drop height, were recalculated. To calculate these values, conservation of energy was assumed; losses due to heat, friction, and sound were neglected. Under realistic conditions, these losses should be factored into the analysis as real-world processes involve energy losses. Another assumption was that minimal deflection would be observed during collisions, which served to further simplify the analysis. If the analysis was to account for large deflections, a thorough understanding of the impact behaviour of both colliding masses would be required. Although these assumptions limit the reliability of the analysis, they allow for baseline values to be determined when comparing the expected and measured behavior of the design.

Equation 4 was used to determine the deflection  $\delta_{dynamic}$  (mm) at minimum height  $h$  (mm), which was set at 50 mm. The equation was developed based on equating the maximum gravitational potential energy (PE) of the steel stock to the maximum elastic potential energy (U) stored in the lattice. Acceleration due to gravity  $g$  was taken to be  $9.81 \frac{m}{s^2}$ . The structural stiffness of the lattice  $K$  (N/mm) was also used in the equation. The mass of the steel round stock  $m$  dropped on the lattice was calculated to be  $2.42 \text{ kg}$  on the density of steel ( $7850 \frac{kg}{m^3}$ ) [4].

$$\delta_{dynamic} = \sqrt{\frac{2mgh}{K}} \quad (4)$$

Similarly, the maximum PE of the block was equated to the maximum kinetic energy (KE) of the block to obtain Equation 5. This equation was used to obtain the impact velocity  $v_i$  (mm/s<sup>2</sup>). The conversion ratio is to convert  $g$  to mm/s<sup>2</sup>.

$$v_i = \sqrt{2gh * \frac{1000mm}{m}} \quad (5)$$

Since small deflections were assumed in the analysis, the maximum force in the lattice  $F_i$  (N) could be determined using Equation 6.

$$F_i = K\delta \quad (6)$$

The time of impact  $t_i$  (s) was determined using the impact velocity and displacement through Equation 7.

$$t_i = \frac{\delta}{v_i} \quad (7)$$

The impact acceleration of the lattice  $a_i$  (m/s<sup>2</sup>) was determined using Equation 8.

$$a_i = \frac{v_i}{t_i} / 1000 \quad (8)$$

The maximum stress and maximum drop height were calculated by assuming that the material would still be within the elastic deformation range. Using this assumption, the ratio of  $\frac{\sigma_{static}}{\delta_{static}}$  using the static testing results could be applied to obtain the desired values. The maximum stress under dynamic loading  $\sigma_{dynamic}$  was determined using Equation 9, and the maximum drop height  $h_{max}$  (in mm) was obtained using the yield stress  $\sigma_{yield}$  with Equation 10. Equation 10 was obtained by substituting  $\sqrt{\frac{2mgh_{max}}{K}}$  in for  $\delta_{max}$  and was rearranging for  $h_{max}$ .

$$\sigma_{dynamic} = \sigma_{static} \left( \frac{\delta_{dynamic}}{\delta_{static}} \right) \quad (9)$$

$$h_{max} = \left( \frac{\delta_{static}}{\sigma_{static}} \sigma_{yield} \right)^2 \left( \frac{K}{2mg} \right) \quad (10)$$

The values used to calculate  $v_i$ ,  $\delta$ ,  $F_i$ ,  $t_i$ ,  $\sigma_{dynamic}$ ,  $a_i$ , and  $h_{max}$  were obtained during the FEA testing of the lattice structures.

Most of the modeled and measured results were within a 1.01% percent difference between each other. Small errors in the dimensions of the lattice could be attributed to printer limitations or human error when using the vernier caliper to take measurements. Significant differences were seen in the material volume, pore volume, porosity, and impact acceleration. The difference in material and pore volume and porosity could be attributed to the presence of support material present within the lattice, which would serve to both increase the volume of the structure and decrease the porosity. The largest difference was in the impact acceleration with a percent difference of 185.23%. This large difference could be since the modelled acceleration assumed 100% energy conservation. The physical testing was influenced by losses, such as friction between the hollow cylinder and the dropped mass, and human error in the exact drop height. The results of future FEA analyses must be adjusted to account for the presence of these errors and inconsistencies. One solution may be to multiply the modeled acceleration by a loss percentage proportional to the losses present in the system.

**Next Steps (design iteration):**

Testing #1 and #2 revealed that the lattice structure performed better than expected. For instance, the acceleration of the block was much smaller than originally determined through FEA. However, multiple aspects of the structure can be re-iterated to improve the design in the context of its application (hockey helmets). To begin, it would be recommended to continue doing FEA analysis, this time, accounting for the orientation of the structure within the helmet and the direction of potential external impacts. This would create a more realistic dynamic testing of the lattice as it aims to mimic its environment of implementation. No further testing or simulation will be conducted for the hexagonal lattice, due to lattice specific values acquired for the FCC/BCC structure during testing. These values would potentially not reflect other structures effectively, which led to the decision to exclude other designs such as the hexagon.

The results of the static and dynamics tests showed the stiffness of the lattice structure itself could be optimized. A decrease in stiffness would allow for a decrease in the acceleration. Because the stiffness is already below the desired target, changing its properties is not necessary but can increase performance even more. For the stiffness to decrease, increasing the porosity of the structure by reducing the amount of support material and/or thinning the trusses is a viable solution. The downside of proceeding with this method is it will increase stress concentrations, and specifically in the zones where the thickness was decreased. Figure 13 shows the iterated lattice with vertical struts of 1 mm thickness instead of 2 mm.

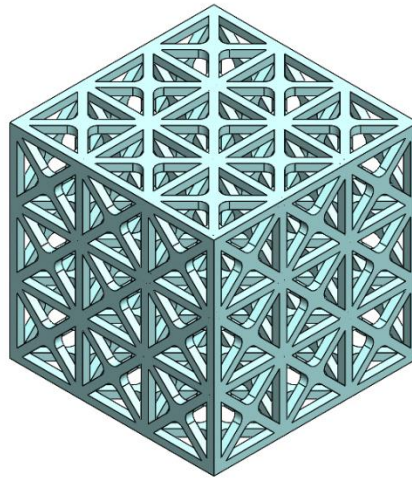


*Figure 13: Isometric view of the iterated lattice of the original BCC/FCC structure, where the internal struts have been reduced in thickness from 2 mm to 1 mm.*

For future recommendations, once the re-iterated lattice is implemented into the new helmet, further testing could be conducted using crash-test mannequins equipped with the helmet. This phase of testing would be implemented towards the later stages of testing.

### **Conclusions To Date:**

The results table at the beginning of the test report provides a comparison of the modelled and measured testing results after using the updated material properties in Table 4. Most of the modelled and measured values did not differ significantly from each other, with the percent

error ranging between 0% to 1.01%. The similarity between the two testing methods will help to increase the validity of future FEA analyses. Differences in volume and porosity can be attributed to the presence of support material. Inconsistencies with the modeled and measured acceleration can be attributed to non-ideal testing conditions such as friction and inaccurate drop height estimation.

To determine the response of the structure under various mesh qualities, a mesh sensitivity analysis was conducted in SolidWorks. A total of 4 mesh qualities were tested on the iterated lattice structure, and the impact on the resultant force and maximum stress was measured. The mesh slider was placed at approximately 20%, 40%, 60%, and 80% along the quality slider bar. The measured values are tabulated in Table 5.

*Table 5: Results of mesh sensitivity analysis on the iterated lattice*

Parameter	Mesh Quality			
	20%	40%	60%	80%
Resultant Force (N)	59.6	59.5	59.4	59.4
Max Stress (MPa)	2.362	2.429	2.45	2.456

From Table 5, both the maximum stress and the resultant force for all tests remains similar, with the 20% quality being slightly less accurate. Therefore, it can be concluded that the iterated lattice is not significantly sensitive to the quality of the mesh. However, to ensure accurate simulation data, at mesh quality of at least 40% should be used. The lattice's low mesh sensitivity allows for future simulations to be completed with lower mesh quality, reducing the time required to run FEA analyses.

An increasing load will be measured and applied to achieve the yield point of the lattice. Given that the design will be used in youth hockey helmets, it is imperative that the lattice will not fail under loading that can be resulted from contact, to ensure protection and reusability. From the results obtained throughout this report, adjustments will be made to improve the design and make it more suitable to the application, including reducing the size of thick interior sections. Adjustments will be made to minimize acceleration on impact, which is the main cause for trauma induced concussions within the game of hockey. In addition, changes can be made to reduce mass of the lattice, which can be done by increasing porosity or reducing the width of certain sections. These changes could improve the performance of the structure without compromising the other performance properties. A controlled iteration process will ensure an improved function of the design.



## References

- [1] "Mechanics of Materials: Strain » Mechanics of Slender Structures," Boston University. Accessed: Mar. 30, 2024. [Online]. Available: <https://www.bu.edu/moss/mechanics-of-materials-strain/>
- [2] "Round bar, rod, wire rod weight. Calculator of the weight of a running meter of metal round bars," Metal Guide. Accessed: Mar. 17, 2024. [Online]. Available: <https://en.metcalc.info/calc-rolled/round/>
- [3] H. H. Calvit, "Experiments on rebound of steel balls from blocks of polymer," *J MECH PHYS SOLIDS*, vol. 15, no. 3, pp. 141–150, May 1967, doi: 10.1016/0022-5096(67)90028-2.
- [4] V. Lapshin and D. Kobzov, "The effect of impact velocity on rebound height after impact interaction," in *IOP Conference Series: Materials Science and Engineering*, in Materials Science and Engineering, vol. 971. IOP Publishing Ltd, Nov. 2020, p. 042015. doi: 10.1088/1757-899X/971/4/042015.
- [5] "Isoflon PMMA Polymethyl-methacrylate," MatWeb. Accessed: Mar. 17, 2024. [Online]. Available: <https://www.matweb.com/search/datasheet.aspx?matguid=e0ba830d1da24d3aa2bd8aa2a6c79f2a>
- [6] "Overview of materials for High Density Polyethylene (HDPE), Injection Molded," MatWeb. Accessed: Mar. 17, 2024. [Online]. Available: [https://www.matweb.com/search/datasheet\\_print.aspx?matguid=fce23f90005d4fbe8e12a1bce53ebdc8](https://www.matweb.com/search/datasheet_print.aspx?matguid=fce23f90005d4fbe8e12a1bce53ebdc8)
- [7] "Stratasys® FDM TPU 92A 3D Printing Polymer." Accessed: Mar. 19, 2024. [Online]. Available: <https://matweb.com/search/DataSheet.aspx?MatGUID=66cb7b618dde4d73850e169f04e3e938&ck=1>

